

Ion transfer voltammetry for analytical screening of fluoroquinolone antibiotics at the water – 1.2-dichloroethane interface

Rudnicki, Konrad; Poltorak, Lukasz; Skrzypek, Sławomira; Sudhölter, Ernst J.R.

DOI

[10.1016/j.aca.2019.07.065](https://doi.org/10.1016/j.aca.2019.07.065)

Publication date

2019

Document Version

Final published version

Published in

Analytica Chimica Acta

Citation (APA)

Rudnicki, K., Poltorak, L., Skrzypek, S., & Sudhölter, E. J. R. (2019). Ion transfer voltammetry for analytical screening of fluoroquinolone antibiotics at the water – 1.2-dichloroethane interface. *Analytica Chimica Acta*, 1085, 75-84. <https://doi.org/10.1016/j.aca.2019.07.065>

Important note

To cite this publication, please use the final published version (if applicable). Please check the document version above.

Copyright

Other than for strictly personal use, it is not permitted to download, forward or distribute the text or part of it, without the consent of the author(s) and/or copyright holder(s), unless the work is under an open content license such as Creative Commons.

Takedown policy

Please contact us and provide details if you believe this document breaches copyrights. We will remove access to the work immediately and investigate your claim.



Ion transfer voltammetry for analytical screening of fluoroquinolone antibiotics at the water – 1,2-dichloroethane interface



Konrad Rudnicki^a, Lukasz Poltorak^{a, b, *}, Stawomira Skrzypek^a, Ernst J.R. Sudhölter^b

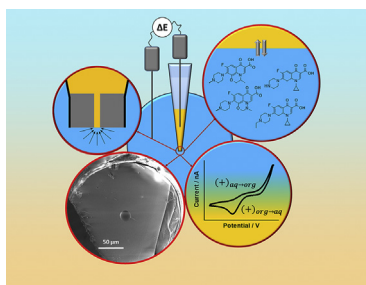
^a Department of Inorganic and Analytical Chemistry, Faculty of Chemistry, University of Lodz, Tamka 12, 91-403, Lodz, Poland

^b Delft University of Technology, Department of Chemical Engineering, Van der Maasweg 9, 2629 HZ, Delft, the Netherlands

HIGHLIGHTS

- Studied fluoroquinolone antibiotics are active at the liquid – liquid interface.
- Liquid – liquid interface miniaturized with fused silica microcapillaries.
- Fluoroquinolone antibiotics give signal at concentration as small as 1 μM .
- Antibiotics $\log P_{\text{DCE}}$ values correlate with calculated $\log P_{\text{octanol}}$ values.
- Ion partition diagrams for all antibiotics are plotted.

GRAPHICAL ABSTRACT



ARTICLE INFO

Article history:

Received 20 February 2019

Received in revised form

6 July 2019

Accepted 30 July 2019

Available online 2 August 2019

Keywords:

ITIES

Polarized liquid – liquid interface

Fluoroquinolone antibiotics

Miniaturization

Ion partition diagrams

ABSTRACT

In this paper, the electrochemical behavior of four fluoroquinolone antibiotics (FAs) [Ciprofloxacin (*Cip*), Enrofloxacin (*Enr*), Marbofloxacin (*Mar*) and Ofloxacin (*Ofl*)] at a polarized interface between two immiscible electrolyte solutions (ITIES) has been studied using ion–transfer voltammetry (ITV). The measurements were conducted in the traditional macroscopic (macro-ITIES) and a recently developed miniaturized (micro-ITIES) platform. The latter was obtained from fused silica microcapillaries having an internal diameter of 25 μm . We used macroITIES to obtain a number of analytical parameters such as: standard Galvani potential of ion transfer ($\Delta\Phi^0$), diffusion coefficients (D), free Gibbs energy of ion transfer (ΔG^0) and partition coefficients ($\log P_{\text{DCE}}$). The latter were compared with the available literature values of $\log P_{\text{octanol}}$. The effect of concentration of the studied antibiotics on the electrochemical response was investigated with the microITIES platform, setting statistical parameters such as: linear dynamic ranges (LDRs – studied from 1 μM up to 50 μM), lower limit of detections (LODs – around 1 μM) and sensitivity (found in the range from $2.6 \cdot 10^{-2}$ to $6.8 \cdot 10^{-2} \text{ nA} \cdot \mu\text{M}^{-1}$). MicroITIES were further used to study the effect of pH on the analytical signal and the results are plotted in a form of ion partition diagrams. Working with microITIES supported with the fused silica capillaries significantly reduced the volumes of consumed chemicals and expedite all analytical experiments. The provided results can be successfully applied in pharmacology and electroanalysis for testing and determination of the chosen fluoroquinolone antibiotics.

© 2019 Elsevier B.V. All rights reserved.

* Corresponding author. Department of Inorganic and Analytical Chemistry, Faculty of Chemistry, University of Lodz, Tamka 12, 91-403, Lodz, Poland.

E-mail addresses: l.poltorak@tudelft.nl, lukasz.poltorak@chemia.uni.lodz.pl (L. Poltorak).

1. Introduction

Fluoroquinolones antibiotics (FAs) exhibit a broad spectrum of

bactericidal activity against gram-positive and gram-negative bacteria. *FAs* inhibit the production of microbial deoxyribonucleic acid (DNA) and ribonucleic acid (RNA) [1]. *FAs* are highly toxic (and at the same time show anticancer activity) and cause degenerative side effects such as damage to the muscle, cartilage and nerve tissues, in extreme situations leading to permanent disability [2]. Consequently, their use in mild infections is not recommended due to frequent and serious side effects [3]. Another general threat is antibiotic resistance of bacteria. This phenomenon is caused by the massive use of antibiotics, which makes their presence in the natural environment disturbingly dangerous [4].

On this ground, it is obvious that *FAs* represent an important class of analytical targets and require constant monitoring in various environments. *FAs* have been investigated using techniques such as diffuse reflectance–Fourier transforms infrared spectroscopy (DR-FTIR) [5], ultra–performance liquid chromatography–tandem mass spectrometry (UPLC–MS/MS) [6] or ultrahigh–performance liquid chromatography–triple quadrupole mass spectrometry (UHPLC–MS/MS/MS) [7] among few others. Electrochemical detection at conventional electrodes via square–wave voltammetry (SWV) [8] or cyclic voltammetry (CV) [8] are other elegant examples. Sensors with electrochemistry based transducing elements are considered to be fast, sensitive, low cost, hold well established miniaturization scenarios and in most cases are environment friendly [9–11]. Furthermore, samples subjected to electrochemical analysis do not require very complicated and complex sample preparation due to low sensitivity to matrix effects.

Electrified liquid – liquid interfaces, also known as the interface between two immiscible electrolyte solutions (ITIES), provide a complementary analytical platform to drugs screening [12]. In electroanalysis, ITIES has a few specific properties: (a) sensing at ITIES is not restricted to reduction or oxidation processes; (b) some electrochemically inactive molecules (at the solid electrodes) can be detected and determined at the ITIES; (c) the electrochemical reactions at the ITIES constitute a key aspect of many (bio)chemical processes occurring in living organisms; (d) systems based on ITIES are relatively cheap, quick and easy to construct whereas (e) the interface itself is considered as renewable and self-healing [13]. Moreover, electrochemical information obtained during ion transfer provides direct insight into drugs partitioning [12,14] that can be further plotted in a form of ion partition diagrams [15,16]. A number of different analytes were successfully detected at the ITIES, ranging from macromolecules (e.g. polyelectrolytes [17], dendrigrafts [18] or proteins [19]) and nanoparticles [20] to small drugs holding a permanently charged or ionisable chemical groups [21]. Antibiotics, like josamycin [22], gentamycin [23] or monensin [24] were frequently used to study so-called facilitated ion transfer reactions, where the antibiotic initially dissolved in the organic phase served as the ionophore for small inorganic cations transferring from the aqueous phase. A number of literature reports show that the ITIES can be comfortably applied to detect biologically active compounds from complex real samples, such as cocaine street samples [25], milk [26], river water [27], plasma [28] or human serum [29], clearly proving its practical utility.

Currently, a constant development in the field of miniaturization of devices is observed. The fabrication of microsensors and automated analytical systems is expected to be the future of electrochemistry and analytical chemistry [30]. Not only practical benefits (decreased volumes of reagents and quantity of materials used) but also superior analytical performance (higher sensitivities and lower limits of detection) are obtained when ITIES was scaled to micro- or nanometer dimensionality [31]. Miniaturized ITIES can be placed into two types of supports: (a) perforated membranes or

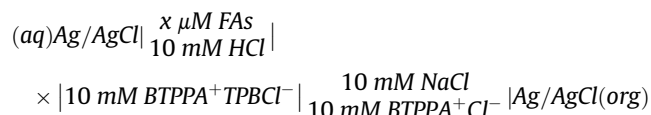
(b) capillaries. The first, are usually prepared using laser ablation or nano/micro lithography processing in thin (polymeric or silicon based) sheets [32,33]. The latter, can be made with the help of dedicated capillary pullers [34] or micro-wire templating methodology [35]. Recently, we have proposed a very simple and cheap method allowing for single pore micro-ITIES preparation using only fused silica capillaries and heat shrinkable micropipette tips [36].

The aim of current work, was the electrochemical investigation of four *FAs* [Ciprofloxacin (*Cip*), Enrofloxacin (*Enr*), Marbofloxacin (*Mar*) and Ofloxacin (*Ofl*)] at the ITIES. To the best of our knowledge their interfacial behavior is here examined for the first time. In this regard we used macro-ITIES and micro-ITIES constructed using fused silica microcapillaries [36] that together with the type of the studied analytes make the novelty of our work. The utilisation of the latter platform allowed for a significant decrease in used chemicals, expedited performed experiments (refreshing macro-ITIES cell is time consuming) and provided improved electroanalytical parameters (higher mass transport to the miniaturized junction). By means of ion transfer voltammetry (ITV) we studied the effect of the pH of the aqueous phase, the *FAs* concentration and the scan rate on the ion transfer behavior of the antibiotics. Extracted partitioning coefficients are discussed in relation to the chemical structure of the studied antibiotics.

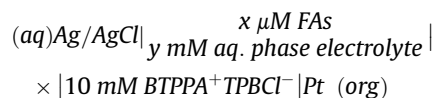
2. Experimental

2.1. Apparatus

All electrochemical studies were performed using an AUTOLAB–PGSTAT 302 N potentiostat–galvanostat (Metrohm Autolab B.V., The Netherlands) controlled by NOVA 1.11.1 software. The experiments at the macro-ITIES were performed using a four electrode configuration in a custom made glass cell. The counter electrodes were made out of rolled Pt wires (the organic phase counter electrode was insulated in a way to prevent its contact with the aqueous phase). The reference electrodes were Ag/AgCl wires. The corresponding Scheme 1 is given below:



The second configuration involves the utilisation of the fused silica capillaries used to support the micro-ITIES We used a two electrode configuration (corresponding to the four electrode system for the macro-ITIES) with the Ag/AgCl as the aqueous phase counter and reference electrode and the Pt wire as the organic phase counter and reference electrode. The scheme of the applied measuring system is presented below (Scheme 2).



The calibration study was performed in the electrochemical cell described in Scheme 2 for $y = 10 \text{ mM HCl}$. The Britton – Robinson buffer was used in order to plot ion partition diagrams. Scanning Electron Microscopy (using a JEOL JSM-6010LA InTouchScope, Tokyo, Japan) was used to image short pieces of microcapillaries. The silica fused micro-capillaries were attached to SEM stage with the carbon tape. Acceleration voltage was set to 5 kV and the working distance was 10 mm.



Scheme 1. Electrochemical cell supporting macro-ITIES.



Scheme 2. Electrochemical cell supporting micro-ITIES.

2.2. Chemicals, reagents and materials

All chemicals used were of analytical reagent grade, *Cip*, *Enr*, *Mar*, *Ofl* were obtained from Sigma-Aldrich (The Netherlands). Fresh stock solutions of *FAs* (10 mM) were prepared in a graduated glass flask by dissolving the appropriate amount of substance in 10 mL of 10 mM hydrochloric acid (HCl) under ultrasound treatment for 15 min. As the organic phase electrolyte, bis(triphenyl phosphoranylidene) ammonium-tetrakis(4-chlorophenyl)borate (BTTPA-TPBCL), and as the aqueous phase electrolyte, 10 mM HCl was used. The BTTPA-TPBCL solution was prepared using bis(triphenylphosphoranylidene)ammonium chloride (BTTPACL, Sigma-Aldrich, 97%) and potassium tetrakis(4-chlorophenyl)borate (KTPBCL, Sigma-Aldrich, 98%). The tetramethylammonium chloride (TMACl, 97%) was used as a reference and model compound.

Britton–Robinson (B–R) buffers (pH 2.0–9.0) were used as the aqueous phase electrolytes in the voltammetric measurements. B–R buffers were prepared from a stock solution of buffer matrix containing 0.04 Mol L⁻¹ of a mixture of boric acid (H₃BO₃), ortho phosphoric acid (H₃PO₄), and acetic acid (CH₃COOH), which was titrated using 0.20 M sodium hydroxide (NaOH) to receive the desired pH values.

All solutions were prepared using mili-Q water or 1,2-dichloroethane and stored in the fridge (ca. 4.0 °C). The chosen organic solvent is sufficiently immiscible with water phase at the same time allowing for the (partial) dissociation of the BTTPA-TPBCL salt. All voltammetric measurements were undertaken at laboratory temperature (22.0 ± 2.0 °C). B–R buffers and HCl solutions were prepared using a glass electrode pH-meter.

Fused silica capillary tubing (295 μm outer diameter and 25 μm internal diameter of pore) was obtained from VWR (The Netherlands).

2.3. Micro-ITIES preparation

A detailed protocol describing the silica fused capillary supporting microITIES preparation is described elsewhere [36]. In brief, a short piece (around 3–5 mm) of methyl deactivated silica fused capillary with an internal diameter of 25 μm was placed at the end of a heat shrinkable micropipette tip. Next, upon very short heating in a Bunsen burner flame, the end of the micropipette tip shrinks, at the same time entrapping the capillary. Tweezers are used to position the capillary within the tip while it is still warm, leaving a shortest possible shank covered with a polymeric casing. The remaining part of the fused silica capillary is removed using a ceramic knife. Throughout all the experiments the capillaries were filled with the organic phase.

3. Results and discussion

3.1. Macro-ITIES

The ion transfer voltammetry at the macro-ITIES was first used

to study the interfacial behavior of all four antibiotics investigated. In Fig. 1 are shown the voltammograms recorded when the pH of the aqueous phase was set to 2 (10 mM HCl) while the organic phase was 10 mM BTTPA-TPBCL dissolved in 1,2-dichloroethane. All antibiotics share similar molecular characteristics, as the presence of a carboxylic group with reported pK_{a1} values ranging from 5.5 to 6.5 [37] on one side of the molecule, and the presence of peripheral nitrogen atoms as part of the piperazine ring with pK_{a2} ≥ 8 [37] on the other side (see Table 1 for more details). Consequently, at pH = 2, the carboxylic acid groups are not dissociated and the piperazine units are protonated, resulting in an overall positively charged antibiotic molecule. In order to transfer positively charged (cationic) molecules from the aqueous to the organic phase, the liquid – liquid interface was polarized from a less to a more positive potential on the forward scan. The process was reversible as seen from the observed integrated current ratios of forward and reversed scan approaching unity (see Fig. 1). The peak-to-peak separation is found to be 73 mV for *Ofl*, 69 mV for *Mar*, 68 mV for *Enr*, and 72 mV for *Cip*. This indicates that all drugs are indeed mono-charged. The deviation of this values from the expected theoretical value of 59 mV · z⁻¹, where z is the molecular charge of the analyte, is commonly observed for electrified liquid – liquid interfaces and originates from the resistive nature of the organic phase [38]. From the scan rate dependency, this is the graphs where the peak current is plotted against the square root of the scan rate (data not shown), and the Randles – Sevcik equation we calculated the diffusion coefficients for all investigated *FAs*. They were found to be in the order of 1 · 10⁻⁶ cm² s⁻¹ for *Mar*, *Cip* and *Enr* and 3.4 · 10⁻⁶ cm² s⁻¹ for *Ofl* (for more details see Table 1). These values are within the expected ranges and are very close to diffusion coefficients of other molecules having similar hydrodynamic dimensionality [25,39].

Another parameter that can be extracted from the ion transfer voltammograms is the standard Galvani potential of the ion transfer ($\Delta_{org}^{aq} \phi^0$), which can be directly related to the molecular hydrophilicity. For cations, the molecules with higher $\Delta_{org}^{aq} \phi_{aq \leftrightarrow org}^0$ exhibit higher hydrophilicity, in other words, more energy has to be supplied to the system to transfer hydrophilic molecule from the aqueous to the organic phase. With this in mind, and the $\Delta_{org}^{aq} \phi^0$ equal to 96; 108; 112 and 185 mV for *Ofl*, *Mar*, *Enr* and *Cip* respectively we see that *Cip* is most hydrophilic antibiotic within this studied molecular family. The $\Delta_{org}^{aq} \phi^0$ can be directly used to calculate the water – 1,2-dichloroethane partition coefficient ($\log P_{DCE}^0$) [38]:

$$\log P_{DCE}^0 = - \frac{\Delta_{org}^{aq} \phi_{antibiotic}^0 z_i F}{2.303RT} \quad (1)$$

where $\Delta_{org}^{aq} \phi_{antibiotic}^0$ is taken from voltammograms whereas z_i , F , R and T have their usual meaning. The $\log P_{DCE}^0$ for antibiotics studied in this work are equal to -3.13, -1.89, -1.82 and -1.62 for *Cip*, *Ofl*, *Mar* and *Enr*, respectively. We have compared these $\log P_{DCE}^0$ values with the corresponding water – octanol partition coefficients

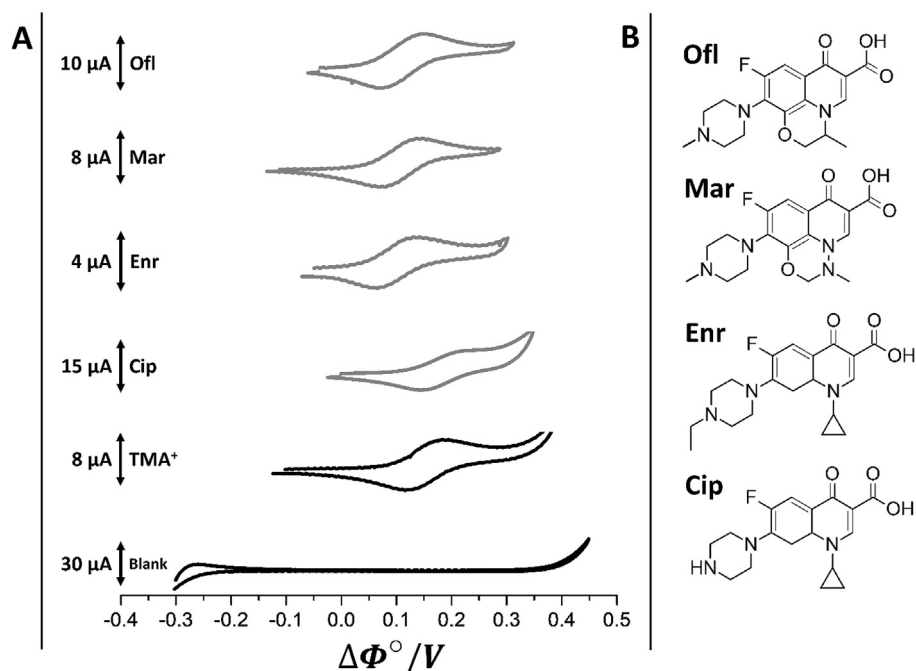


Fig. 1. A – Ion transfer voltammograms for all studied antibiotics (grey), TMA⁺ and a blank experiment (black) recorded at macro-ITIES. B – Molecular structures of the studied antibiotics. Conditions: scan rate = 10 mV s⁻¹; [antibiotics or TMA⁺] = 50 μM; The aqueous phase was set to a pH = 2.

Table 1

The summary of physico-chemical and electro-analytical properties pertaining to studied FAs.

Analyte name	z	pK_{a1} [37]	pK_{a2} [37]	K_D^a	$pH_{[H-X]_{aq}^+=[X]_{org}}$ ^b	D [cm ² s ⁻¹]	$\Delta G_{Analyte}^{0, aq \rightarrow org}$ / [kJ mol ⁻¹] ^c	$\Delta_{org}^{aq} \Phi^0_{Analyte}$ [mV]	$\log P_{DCE}^0$ ^d	Sensitivity [nA μM ⁻¹] ^e	LOD [μmol/l] ^f
TMA⁺	1	–	–	–	–	13.6×10^{-6} [41]	15.4	160	-2.71	$a_f = 1.18 \times 10^{-2}$ $a_r = 1.39 \times 10^{-2}$	1.06 2.03
Mar	1	5.69	8.02	0.3	5.6	1.48×10^{-6}	10.4	108	-1.82	$a_f = 3.21 \times 10^{-3}$ $a_r = 6.23 \times 10^{-3}$	0.52 1.08
Ofi	1	5.98	8.00	0.15	5.8	3.40×10^{-6}	10.8	112	-1.89	$a_f = 2.85 \times 10^{-3}$ $a_r = 6.23 \times 10^{-3}$	1.04 1.25
Cip	1	6.14	8.85	0.3	6.4	0.62×10^{-6}	17.9	185	-3.13	$a_f = 5.53 \times 10^{-3}$ $a_r = 6.82 \times 10^{-3}$	1.15 0.65
Enr	1	6.20	8.13	1.5	5.0	0.80×10^{-6}	9.3	96	-1.62	$a_f = 2.62 \times 10^{-3}$ $a_r = 5.21 \times 10^{-3}$	3.21 1.32

^a See eq. (6).

^b pH indicated with black arrow in Fig. 5.

^c Calculated using $\Delta G_{drug}^{0, aq \rightarrow org} = zF\Delta_{org}^{aq} \Phi^0_{drug}$.

^d Calculated using eq. (1).

^e a_f and a_r correspond to the forward and reverse slope of the calibration curve.

^f Calculated using eq. (4).

($\log P_{octanol}$) available in the literature (see Table 2).

We found that for all FA antibiotics the discrepancy between different $\log P_{octanol}$ data found in the literature is very high (e.g. the experimental values for Cip are found in the range between -0.13 and -1.51) even though identical experimental conditions were used during experiments. The set of $\log P_{octanol}$ that gave good correlation with the $\log P_{DCE}^0$ from this work is shown in Fig. 2 and correspond to values calculated based on the method reported elsewhere [40]. Most of the reports tabulated in Table 2 points that Cip is the most hydrophilic, Enr is the most hydrophobic with Ofi and Mar being located somewhere in between. This example proves that the reproducibility of seemingly straightforward shake flask experiments is rather low and points at significant differences in the calculated values. In contrary, the $\log P_{DCE}^0$ calculated using parameters obtained at ITIES seems to be much more reliable since $\Delta_{org}^{aq} \Phi^0$ is the inherent parameter of each interfacially active

molecule. The $\Delta_{org}^{aq} \Phi^0$ were additionally used to calculate the standard Gibbs energy of ion transfer reaction ($\Delta G_{drug}^{0, aq \rightarrow org}$) according to:

$$\Delta G_{drug}^{0, aq \rightarrow org} = zF\Delta_{org}^{aq} \Phi^0 \quad (2)$$

where z and F is the charge and Faraday constant respectively. Resulting $\Delta G_{drug}^{0, aq \rightarrow org}$ are summarized in Table 1.

We used macro-ITIES in order to describe the number of analytical parameters related to studied FA antibiotics. The utilisation of the glass cell supporting the macro-ITIES is association with very few practical obstacles: (i) it requires frequent refreshing when the composition of one of the phases is changed; (ii) it consumes significant amount of chemicals (especially the toxic organic phase) or (iii) exclude convective stirring due to arrangement of Luggin capillaries. For these reasons, following experiments were

Table 2
Literature values for the Octanol/water partition coefficients for studied FAs.

FA's				pH	Ref
<i>Ofl</i>	<i>Cip</i>	<i>Mar</i>	<i>Enr</i>		
-1.06	-1.51	–	–	7.0	[45]
-0.44	-1.11	–	–	7.4	[46]
0.02	–	–	–	7.4	[47]
–	-0.13	–	–	7.0	[48]
–	-0.75	–	–	7.0	[49]
–	-1.10	-0.99	0.23	7.4	[50]
–	-1.10	-1.16	0.55	-7.0	[51]
–	–	3.48	–	7.0	[52]
–	–	-0.76	–	7.4	[53]
–	–	-1.11	0.70	–	[54], (a)
–	–	–	0.70	–	[55], (b)
-0.02	-0.57	-0.53	0.58	–	[56], (c)
-0.26	-0.70	-0.63	0.27	–	(d)
2.49	2.24	2.15	2.58	–	[57], (e)
-0.39	-1.08	-0.49	-0.25	–	
1.20	1.18	-0.21	1.91	–	
0.98	1.28	1.45	1.75	–	
1.47	1.90	0.36	2.21	–	

(a) Calculated using EPI Suite v. 3.20 algorithm.

(b) Taken from ChemSpider Database, <http://www.chemspider.com>.

(c) Taken from <http://www.vcclab.org/lab/alogps/>.

(d) Taken from <https://www.molinspiration.com/>.

(e) Taken from <http://www.swissadme.ch/>.

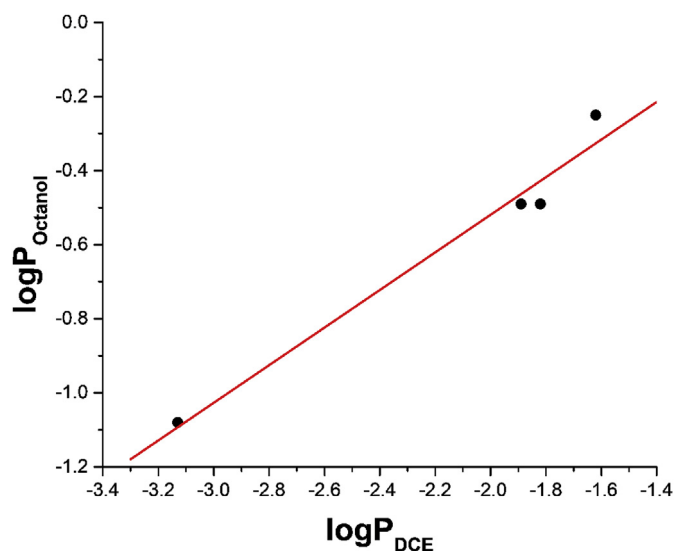


Fig. 2. Correlation between $\log P_{DCE}$ values obtained experimentally and calculated $\log P_{Octanol}$ taken from Ref. [40]. The goodness of fit, $R^2 = 0.956$.

performed using micro-ITIES formed using silica fused microcapillaries. These platforms, not only solve mentioned practical impediments, but also improve electroanalytical performance.

3.2. Micro-ITIES

Recently we have developed an easy, cheap and very simple ITIES miniaturization technique that is based on the use of fused silica capillaries. These capillaries come with different internal wall surface chemistries (hydrophilic or hydrophobic and allow for an aqueous or an organic phase filling, respectively) and they are all commercially available having pore diameters as small as 5 μm . For the current study, we used fused silica capillaries of 25 μm diameter

with the interior of the walls terminated with (hydrophobic) methyl functionalities. The capillaries were filled with the 10 mM BTPPA-TPBCl dissolved in 1,2-dichloroethane and then contacted with 10 mM aqueous HCl solution (pH = 2) containing the antibiotic of interest. These conditions are similar as used in the experiments described before using the macro-ITIES set-up. In Fig. 3 is shown the ion transfer voltammogram as recorded in the presence of 30 μM TMA^+Cl^- dissolved in the aqueous phase, as our model compound. By sweeping the potential from a lower to a higher voltage and then return to the lower potential values, it is observed that TMA^+ undergoes a reversible ion transfer reaction. Due to the micrometer dimensionality, and the relatively thick pore walls, the voltammograms exhibit very unique and also asymmetric characteristics. On the forward scan, thus while TMA^+ transfer from the aqueous to the organic phase, the mass transfer of the analyte to the interface is not limited by only linear diffusion, but is found to be enhanced, likely as a result of the established hemispherical diffusion zones (see Fig. 3 inset B) This results in the characteristic signal shaped as sigmoidal wave. In the backward scan the peak-shaped signal is recorded indicating that the ion transfer process is limited by linear diffusion. This is indeed the case, as the TMA^+ transfer from the organic phase present in the narrow and lengthy pore (see drawings on Fig. 3C for visualization). From the Faradaic current extracted from the forward sigmoidal wave (steady-state current) we can calculate the electroactive interface area and see how it correlates with the pore dimensionality found with imaging techniques. For this reason we use the Saito equation describing the steady state current at the micro-disc electrode, assuming the description is also valid for the ITIES:

$$I_{ss} = 4zDCFr \quad (3)$$

where I_{ss} is the steady-state current, z is the charge of an analyte, D is the aqueous phase diffusion coefficient, F is the Faraday constant and r is the capillary radius, one can estimate the dimensionality of the electroactive surface area. By simple rearrangement of eq. (1), with D equal to $13.8 \cdot 10^{-6} \text{cm}^2 \text{s}^{-1}$ [41], $[\text{TMA}^+] = 30 \mu\text{M}$ and I_{ss}

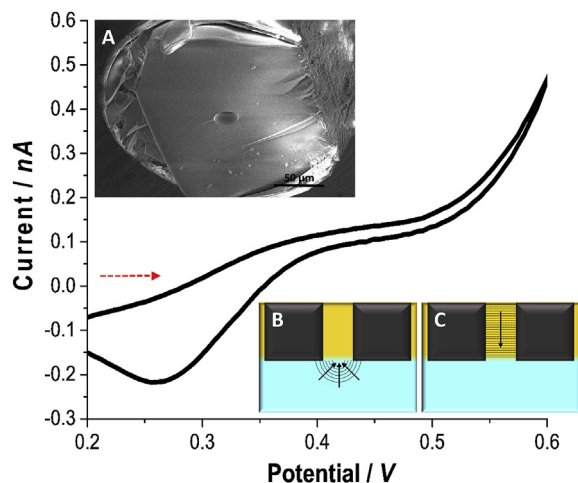


Fig. 3. Ion transfer voltammogram of $[TMA^+] = 30 \mu\text{M}$ initially present in the aqueous phase of $\text{pH} = 2$ (to 10 mM HCl) recorded at micro-ITIES supported with a fused silica capillary with a pore diameter of $25 \mu\text{m}$. Insets: A – is the SEM image of the capillary used to support ITIES; B – represents the hemispherical mass transfer of $TMA_{aq \rightarrow org}^+$ and C – depicts the linear mass transfer of $TMA_{org \rightarrow aq}^+$. Forward polarization is indicated with red dashed arrow. (For interpretation of the references to colour in this figure legend, the reader is referred to the Web version of this article.)

equal to 0.18 nA we calculate $22.5 \mu\text{m}$ as the pore diameter. This number is very close to a diameter of $24 \mu\text{m}$ as was obtained from the SEM micrograph (see the inset A in Fig. 3). A good correlation between the pore diameter obtained from ion transfer voltammetry and direct pore imaging indicates that the liquid – liquid interface is indeed positioned on the pore ingress. Any organic phase leakage from the pore or entrance of the aqueous phase into the pore can therefore be excluded.

The single pore micro-ITIES prepared and characterized in this manner were used next to study the effect of concentration of studied FAs on electrochemical response. The observed ion transfer voltammograms for *Cip*, *Enr* and *Mar*, taken at an aqueous solution $\text{pH} = 2$, are shown in Fig. 4A–C respectively. A similar voltammogram for *Ofl* was already published [36]. Again, due to the asymmetric diffusion layer profile, we observe here a sigmoidal signal on the antibiotic transfer from the aqueous to the organic phase and peak-shaped signal on the back transfer. It seems that for the *Enr*, on the back transfer two overlaid peaks are present, which may indicate the interfacial adsorption/desorption process – common for bulky molecules [42]. The limit of detection for all antibiotics was calculated using following expression:

$$LOD = \frac{3.3S_d}{S} \quad (4)$$

where S is the slope of the calibration curve and S_d is the standard error of the calibration curve fitting intercept. Calculated LOD values (see Table 1 for details) for our studied antibiotics fluctuate around $1 \mu\text{M}$ and this is in agreement with the lowest measured concentration of $1 \mu\text{M}$. Interestingly, the sensitivity of the voltammetric detection differs for the forward and backward scan, being always higher for the latter. The ratio between forward and backward scan equals to 1.9 for *Mar*; 2.0 for *Enr*; 1.2 for *Cip* and as reported previously 2.2 for *Ofl* [36]. The calculated value for *Cip* is an estimate rather than a true value since the transfer of *Cip* from the aqueous to the organic phase was overlaid with the limiting current on the positive side of the potential window arising from $H_{aq \rightarrow org}^+$. For the TMA^+ cation this ratio was close to 1 (raw data not shown). This indicates that the pre-concentration (stripping from the

aqueous phase) occurs only for all FAs, and not for TMA^+ . The factors that may collectively contribute to the observed increased reverse sensitivity include: (i) a lower diffusion of a molecule in the organic phase; (ii) the confined geometry of a lengthy pore inducing the “crowding effect” or (iii) the interactions (such as van der Waals and hydrophobic interactions) between antibiotics and methyl group present at the internal wall surface. Similar observation were made by Alvarez de Eulate et al. [43] for conical shaped pores.

The micro-ITIES were further used to study the mechanism of the FAs interfacial ion transfer reactions at different pH values. The plots of standard ion transfer potential versus the pH of the aqueous phase are known as ion partition diagrams. These, for studied antibiotics, are presented in Fig. 5. In present study, the pH dependent mechanism behind the recorded ionic currents is common to all four drugs and can be directly deduced from ion partition diagrams. Studied antibiotics possess two functionalities that can be protonated/deprotonated within conventional pH scale. These are the carboxylic group (with pK_{a1} for *Mar*, *Enr*, *Ofl* and *Cip* equal to 5.69, 6.20, 5.98 and 6.14 respectively) and amine group within piperazine ring (with pK_{a2} for *Mar*, *Enr*, *Ofl* and *Cip* equal to 8.02, 8.13, 8.00 and 8.85 respectively) – these values are also present in Table 1. Consequently, we can distinguish four antibiotic speciation forms, which occurrence is governed by the aqueous phase pH: (i) the cation with fully protonated amine group and non-dissociated carboxylic group for $\text{pH} < pK_{a1}$ and $\text{pH} < pK_{a2}$; (ii) the zwitterion with protonated amine group and dissociated carboxylic group for the $pK_{a1} > \text{pH} < pK_{a2}$; (iii) the neutral form with the deprotonated amine group and non-dissociated carboxylic group for the $pK_{a1} > \text{pH} < pK_{a2}$ and finally (iv) the anion in a form of fully deprotonated molecule for the $\text{pH} > pK_{a1}$ and $\text{pH} > pK_{a2}$. For the acidic pH region up to around 5–6 (slightly oscillates depending from the FAs pK_{a1}) all drugs are positively charged and undergoes electrochemically controlled reversible interfacial ion transfer reaction (schematically shown in Figs. 6–1). By increasing the pH of the aqueous phase we change the antibiotic speciation and the electrochemical nature of the recorded signal which can be described with the following relationship [44]:

$$\Delta_{org}^{aq} \phi_{1/2} = \Delta_{org}^{aq} \phi_{drug}^0 + \frac{RT}{F} \left(\frac{10^{-\text{pH}} + K_a + K_a K_D}{10^{-\text{pH}}} \right) \quad (5)$$

where $\Delta_{org}^{aq} \phi_{1/2}$ is the half wave potential and K_D is defined as ratio between the neutral form of the antibiotic in the aqueous and the organic phase:

$$K_D = \frac{[Drug]_{aq}^{+/- \text{ or } 0}}{[Drug]_{org}^{+/- \text{ or } 0}} \quad (6)$$

Using eq. (6), with K_D as the adjustable variable, the fitting (red, dashed line) to the data points from Fig. 5 was performed. At the pH indicated with the black arrow (5.0; 5.6; 5.8 and 6.4 for *Enr*; *Mar*; *Ofl* and *Cip* respectively) the concentration of protonated and positively charged antibiotic species in the aqueous phase are equal to the concentration of neutral drug species in the organic phase, this is $[H\text{-Antibiotic}^+]_{aq} = [\text{Antibiotic}]_{org}$.

As the pH of the aqueous phase increases and goes beyond pK_{a1} , the $\Delta_{org}^{aq} \phi_{1/2}$ shifts to more positive potential values. This is observed for all antibiotics investigated. The faradaic currents recorded from this point until $\text{pH} \sim 9$ are governed by the facilitated transfer of proton from the aqueous to the organic phase (forward scan) as schematically shown in Figs. 6–2. In other words, the non-protonated amine group (dissociation of carboxylic group in the 1,2-dichloroethane is less probable) acts as the proton complexing

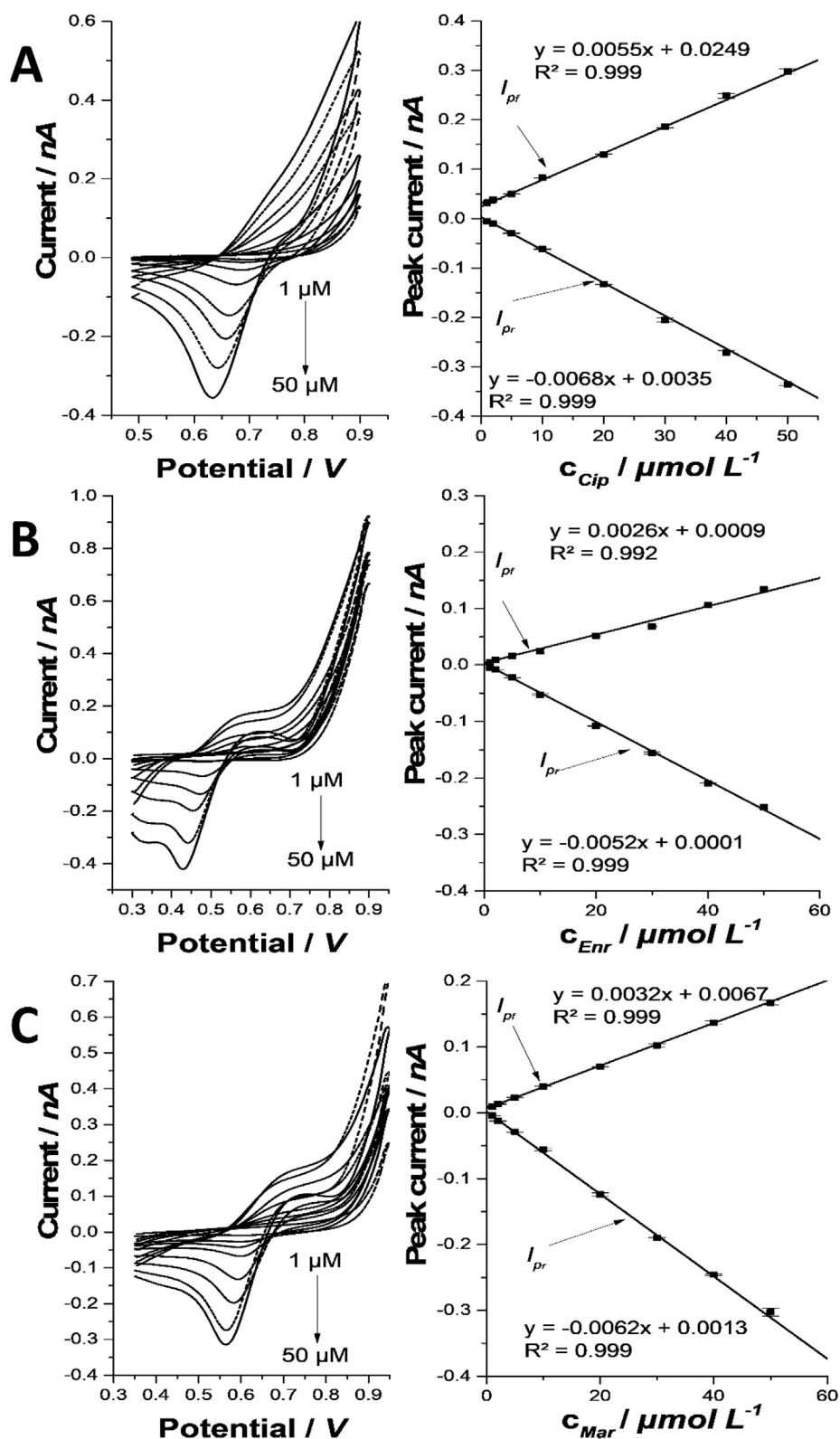


Fig. 4. Ion transfer voltammograms recorded for increasing antibiotic concentrations of 1, 2, 5, 10, 20, 30, 40 and 50 μM at $\text{pH} = 2$ (left panel), together with the forward and reverse currents intensities in function of antibiotics concentration (calibration curves, for $n = 8$) as shown in the right panel. Linear fit, together with the linear fit equation and fitting goodness are also reported. A, B and C corresponds to Cip, Enr and Mar respectively.

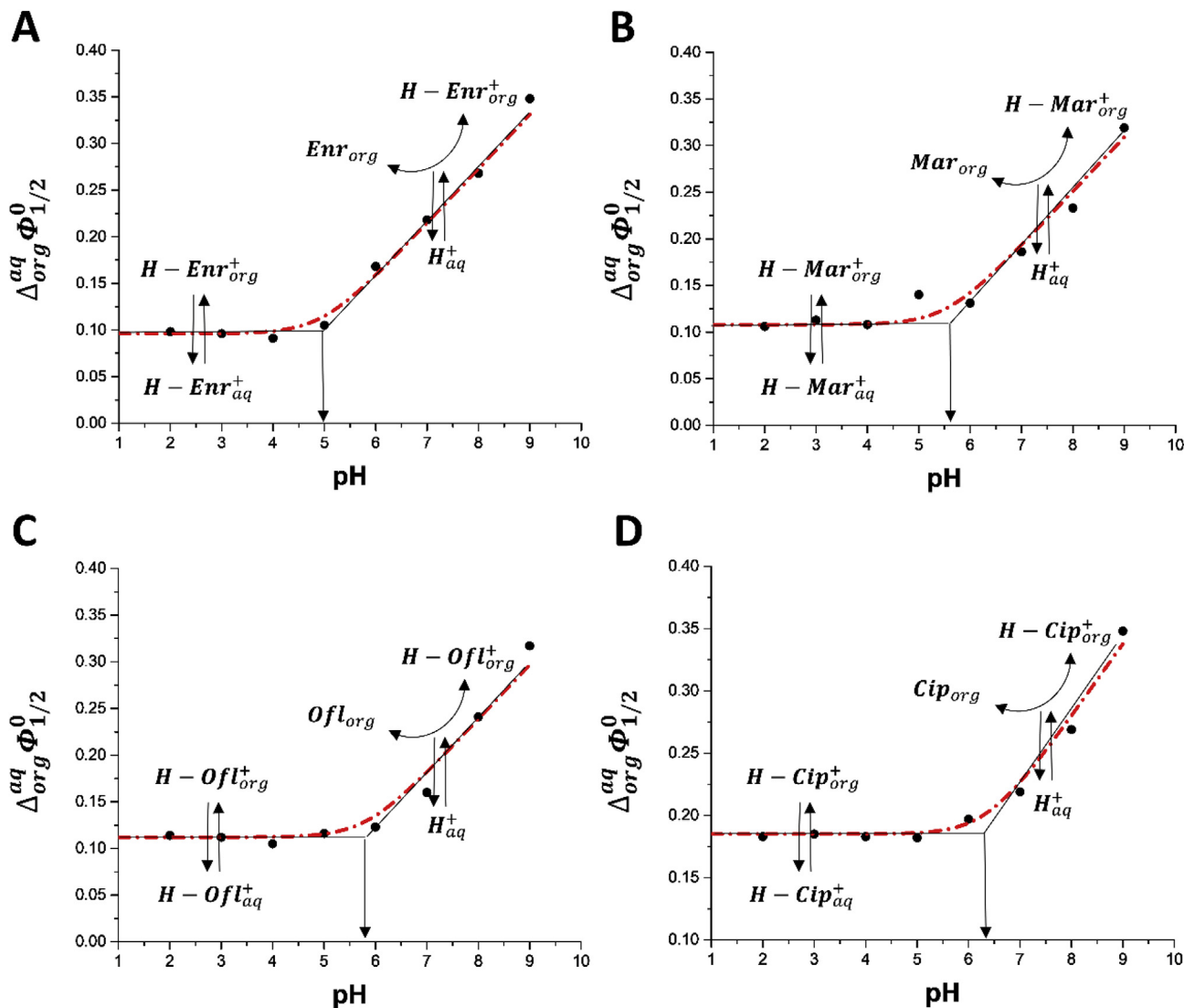


Fig. 5. Ion partition diagrams for A – Enr; B – Mar; C – Ofl and D – Cip. Red dashed line is the best fit to the experimental data using eq. (5). (For interpretation of the references to colour in this figure legend, the reader is referred to the Web version of this article.)

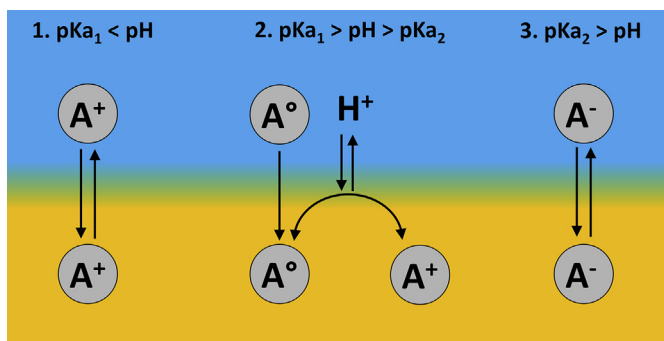


Fig. 6. Schematic representation of the pH dependent ion transfer mechanism common for all studied antibiotics. A stands for antibiotic.

agent. Further increase of the solution pH (>9 and up to 11) showed voltammograms with no signal within the available potential window. Most probably, the interfacial transfer of the anionic form of the antibiotics (Figs. 6–3) occurs beyond the transfer of the

anionic part of the aqueous phase background electrolyte. All parameters extracted from ion partition diagrams are additionally summarized in Table 1.

4. Conclusions

In this work we performed a comprehensive electroanalytical description of four fluoroquinone antibiotics (enrofloxacin, marbofloxacin, ofloxacin and ciprofloxacin) at the electrified liquid – liquid interface. The experiments were performed using two platforms: (i) conventional four electrode glass cell supporting a macroscopic electrified liquid – liquid interface and (ii) the method developed by us where the electrified liquid – liquid interface was supported with fused silica microcapillaries. We found that all studied molecules give signals within the available potential window with ciprofloxacin being the most hydrophilic compound among all studied substances. The electroanalytical characterization revealed that the lower limit of detection is around 1 μ M. Moreover, we conclude that the electrified liquid – liquid interface can serve as a sensors to detect a family of fluoroquinone antibiotics rather than single entities – due to similar structures these drugs

undergoes interfacial ion transfer at similar potential values. We did not find the expected correlation between the water – 1,2-dichloroethane antibiotics partition coefficient and the water – Octanol partition coefficient. This is due to the immense discrepancy found in published literature data, rather than uncertainties from our experimental results. This observation only underlies the utility of the electrified liquid – liquid interface when it comes to partition coefficient evaluation. We are currently developing a set of new, simple and low-cost miniaturization techniques with the primary application in electroanalysis. As a sequel of these work we will target other drugs and biologically relevant chemicals.

Declaration of competing interest

The authors declare that they have no known competing financial interests or personal relationships that could have appeared to influence the work reported in this paper.

Acknowledgements

The authors acknowledge financial support from the University of Lodz, Poland (Grant No. B1811100001859.02). K.R. acknowledge the financial support of the National Science Center (NCN) in Cracow, Poland (Grant no. UMO–2018/29/N/ST4/01054). K.R. is grateful for the funding obtained from the Erasmus+ program.

Appendix A. Supplementary data

Supplementary data to this article can be found online at <https://doi.org/10.1016/j.aca.2019.07.065>.

References

- [1] (n.d.), <http://www.fda.gov/Drugs/DrugSafety/ucm511530.htm>.
- [2] L. Riaz, T. Mahmood, A. Khalid, A. Rashid, M.B. Ahmed Siddique, A. Kamal, M.S. Coyne, Fluoroquinolones (FQs) in the environment: a review on their abundance, sorption and toxicity in soil, *Chemosphere* 191 (2018) 704–720, <https://doi.org/10.1016/j.chemosphere.2017.10.092>.
- [3] X. Van Doorslaer, J. Dewulf, H. Van Langenhove, K. Demeestere, Fluoroquinolone antibiotics: an emerging class of environmental micropollutants, *Sci. Total Environ.* 500–501 (2014) 250–269, <https://doi.org/10.1016/j.scitotenv.2014.08.075>.
- [4] A. Ezzariai, M. Hafidi, A. Khadra, Q. Aemig, L. El Fels, M. Barret, G. Merlina, D. Patureau, E. Pinelli, Human and veterinary antibiotics during composting of sludge or manure: global perspectives on persistence, degradation, and resistance genes, *J. Hazard Mater.* 359 (2018) 465–481, <https://doi.org/10.1016/j.jhazmat.2018.07.092>.
- [5] R. Kurrey, M. Mahilang, M. Kanti Deb, J. Nirmalkar, K. Shrivastava, S. Pervez, M. Kumar Rai, J. Rai, A direct DRS-FTIR probe for rapid detection and quantification of fluoroquinolone antibiotics in poultry egg-yolk, *Food Chem.* 270 (2019) 459–466, <https://doi.org/10.1016/j.foodchem.2018.07.129>.
- [6] S.K. Saxena, R. Rangasamy, A.A. Krishnan, D.P. Singh, S.P. Uke, P.K. Malekadi, A.S. Sengar, D.P. Mohamed, A. Gupta, Simultaneous determination of multi-residue and multi-class antibiotics in aquaculture shrimps by UPLC-MS/MS, *Food Chem.* 260 (2018) 336–343, <https://doi.org/10.1016/j.foodchem.2018.04.018>.
- [7] J. Kazakova, R. Fernández-Torres, M. Ramos-Payán, M.Á. Bello-López, Multi-residue determination of 21 pharmaceuticals in crayfish (*Procambarus clarkii*) using enzymatic microwave-assisted liquid extraction and ultrahigh-performance liquid chromatography-triple quadrupole mass spectrometry analysis, *J. Pharm. Biomed. Anal.* 160 (2018) 144–151, <https://doi.org/10.1016/j.jpba.2018.07.057>.
- [8] K.R. Reddy, P.K. Brahman, L. Suresh, Fabrication of high performance disposable screen printed electrochemical sensor for ciprofloxacin sensing in biological samples, *Meas. J. Int. Meas. Confed.* 127 (2018) 175–186, <https://doi.org/10.1016/j.measurement.2018.05.078>.
- [9] K. Rudnicki, S. Domagała, B. Burnat, S. Skrzypek, Voltammetric and corrosion studies of the ionophoric antibiotic–salinomycin and its determination in a soil extract, *J. Electroanal. Chem.* 783 (2016) 56–62, <https://doi.org/10.1016/j.jelechem.2016.10.058>.
- [10] K. Rudnicki, P. Landová, M. Wrońska, S. Domagała, J. Čáslavský, M. Vávrová, S. Skrzypek, Quantitative determination of the veterinary drug monensin in horse feed samples by square wave voltammetry (SWV) and direct infusion electrospray ionization tandem mass spectrometry (DI–ESI–MS/MS), *Microchem. J.* 141 (2018) 220–228, <https://doi.org/10.1016/j.microc.2018.05.032>.
- [11] M. Brycht, O. Vajdle, K. Sipa, J. Robak, K. Rudnicki, J. Piechocka, A. Tasić, S. Skrzypek, V. Guzsány, β -Cyclodextrin and multiwalled carbon nanotubes modified boron-doped diamond electrode for voltammetric assay of carbendazim and its corrosion inhibition behavior on stainless steel, *Ionics* 24 (2017) 923–934, <https://doi.org/10.1007/s11581-017-2253-0>.
- [12] Z. Samec, *Electrochemistry at the interface between two immiscible electrolyte solutions* (IUPAC technical report), *Pure Appl. Chem.* 76 (2004) 2147–2180.
- [13] D. Fermi, H.J. Lee, H.H. Girault, F. Reymond, D. Fermin, Electrochemistry at liquid/liquid interfaces: methodology and potential applications, *Electrochim. Acta* 45 (2000) 2647–2662, <http://linkinghub.elsevier.com/retrieve/pii/S0013468600003431>.
- [14] K. Kontturi, L. Murtomäki, Electrochemical determination of partition coefficients of drugs, *J. Pharm. Sci.* 81 (1992) 970–975.
- [15] V. Chopineaux-Courtois, F. Reymond, G. Bouchard, P.A. Carrupt, B. Testa, H.H. Girault, Effects of charge and intramolecular structure on the lipophilicity of nitrophenols, *J. Am. Chem. Soc.* 121 (1999) 1743–1747, <https://doi.org/10.1021/ja9836139>.
- [16] S.A. Dassie, Facilitated proton transfer or protonated species transfer reactions across oil/water interfaces, *J. Electroanal. Chem.* 728 (2014) 51–59, <https://doi.org/10.1016/j.jelechem.2014.06.020>.
- [17] L. Zhang, Y. Kitazumi, T. Kakiuchi, Potential-dependent adsorption and transfer of poly(diallyldialkylammonium) ions at the nitrobenzene/water interface, *Langmuir* 27 (2011) 13037–13042, <https://doi.org/10.1021/la2028077>.
- [18] G. Herzog, S. Flynn, C. Johnson, D.W.M. Arrigan, Electroanalytical behavior of poly-L-lysine dendrigrafts at the interface between two immiscible electrolyte solutions, *Anal. Chem.* 84 (2012) 5693–5699.
- [19] D.W.M. Arrigan, G. Herzog, M.D. Scanlon, J. Strutwolf, Bioanalytical applications of electrochemistry at liquid-liquid microinterfaces, *Electroanal. Chem., A Ser. Adv.* 25 (2013) 105–178.
- [20] T.J. Stockmann, L. Angelé, V. Brasiliense, C. Combellas, F. Kanoufi, Platinum nanoparticle impacts at a Liquid/Liquid interface, *Angew. Chem. Int. Ed.* 56 (2017) 13493–13497, <https://doi.org/10.1002/anie.201707589>.
- [21] H. Alemu, Voltammetry of drugs at the interface between two immiscible electrolyte solutions, *Pure Appl. Chem.* 76 (2004) 697–705, <https://doi.org/10.1351/pac200476040697>.
- [22] E. V. Vladimirova, A.A. Dunaeva, E. V. Shipulo, O.M. Petrukhin, M. V. Kostitsyna, Studies of complex formation between macrolide antibiotics and alkali and alkali – earth metals by the voltammetry at the interface of two immiscible, *Electrolyte Solut.* 47 (2011) 384–391, <https://doi.org/10.1134/S1023193510121031>.
- [23] O.M. Petrukhin, M. V. Kostitsyna, T.G. Dzherayan, E. V. Shipulo, E. V. Vladimirova, A.A. Dunaeva, Complexation of aminoglycoside antibiotics with metal cations as a derivatization Reaction: determination of gentamicin by equilibrium electrochemical and spectrophotometric, *Methods* 64 (2009) 975–981, <https://doi.org/10.1134/S1061934809090135>.
- [24] S.A. Dassie, A.M. Baruzzi, Comparative Analysis of Alkali and Alkaline-Earth Cation Transfer Assisted by Monensin across the Water 1,2-dichloroethane Interface, vol. 492, 2000, pp. 94–102.
- [25] L. Poltorak, I. Eggink, M. Hoitink, E.J.R. Sudholter, M. De Puit, Electrified soft interface as a selective sensor for cocaine detection in street samples, *Anal. Chem.* 90 (2018) 8–13, <https://doi.org/10.1021/acs.analchem.8b00916>.
- [26] S. Jeshycka, E.M. Kim, H.J. Lee, Electrochemical investigation on ionizable levofloxacin transfer reaction across liquid/liquid interfaces and potential applications to milk analysis, *Electrochim. Acta* 282 (2018) 964–972, <https://doi.org/10.1016/j.electacta.2018.07.018>.
- [27] S. Jeshycka, H.Y. Han, H.J. Lee, Voltammetric understanding of ionizable doxorubicin transfer reactions across liquid/liquid interfaces and sensor development, *Electrochim. Acta* 245 (2017) 211–218, <https://doi.org/10.1016/j.electacta.2017.05.096>.
- [28] J.A. Ribeiro, S. Benfeito, F. Cagide, J. Teixeira, P.J. Oliveira, F. Borges, A.F. Silva, C.M. Pereira, Electrochemical behaviour of a novel mitochondria-targeted antioxidant at an ITIES: an alternative approach to study lipophilicity, *Anal. Chem.* (2018), <https://doi.org/10.1021/acs.analchem.8b00787>.
- [29] H.R. Kim, C.M. Pereira, H.Y. Han, H.J. Lee, Voltammetric studies of toptecan transfer across liquid/liquid interfaces and sensing applications, *Anal. Chem.* 87 (2015) 5356–5362, <https://doi.org/10.1021/acs.analchem.5b00653>.
- [30] F.T.G. van den Brink, W. Olthuis, A. van den Berg, M. Odijk, Miniaturization of electrochemical cells for mass spectrometry, *TrAC Trends Anal. Chem.* (Reference Ed.) 70 (2015) 40–49, <https://doi.org/10.1016/j.trac.2015.01.014>.
- [31] L. Poltorak, A. Gamero-Quijano, G. Herzog, A. Walcarius, Decorating soft electrified interfaces: from molecular assemblies to nano-objects, *Appl. Mater. Today* 9 (2017) 533–550, <https://doi.org/10.1016/j.apmt.2017.10.001>.
- [32] S. Peulon, V. Guillou, M. L'Her, Liquid/liquid microinterface. Localization of the phase boundary by voltammetry and chronoamperometry; influence of the microchannel dimensions on diffusion, *J. Electroanal. Chem.* 514 (2001) 94–102, [https://doi.org/10.1016/S0022-0728\(01\)00617-9](https://doi.org/10.1016/S0022-0728(01)00617-9).
- [33] R. Zazpe, C. Hibert, J. O'Brien, Y.H. Lanyon, D.W.M. Arrigan, Ion-transfer voltammetry at silicon membrane-based arrays of micro-liquid-liquid interfaces, *Lab Chip* 7 (2007) 1732–1737, <https://doi.org/10.1039/b712601h>.
- [34] N.T. Iwai, M. Kramaric, D. Crabbe, Y. Wei, R. Chen, M. Shen, GABA detection with nano-ITIES pipet electrode: a new mechanism, water/DCE–octanoic acid interface, *Anal. Chem.* 90 (2018) 3067–3072, <https://doi.org/10.1021/acs.analchem.7b03099>.

- [35] T.J. Stockmann, Z. Ding, Hydrophobicity of room temperature ionic liquids assessed by the Galvani potential difference established at micro liquid/liquid interfaces, *J. Electroanal. Chem.* 649 (2010) 23–31, <https://doi.org/10.1016/j.jelechem.2009.12.024>.
- [36] K. Rudnicki, L. Poltorak, S. Skrzypek, E.J.R. Sudhölter, E.J.R. Sudholter, Fused silica micro-capillaries used for a simple miniaturization of the electrified liquid – liquid interface, *Anal. Chem.* 90 (2018) 7112–7116, <https://doi.org/10.1021/acs.analchem.8b01351>.
- [37] X. van Doorslaer, *Advanced Oxidation of Uoroquinolone Antibiotics in Water by Heterogeneous Photocatalysis*, PhD thesis, 2014.
- [38] L. Poltorak, E.J.R. Sudhölter, L.C.P.M. de Smet, Effect of charge of quaternary ammonium cations on lipophilicity and electroanalytical parameters: task for ion transfer voltammetry, *J. Electroanal. Chem.* 796 (2017), <https://doi.org/10.1016/j.jelechem.2017.04.051>.
- [39] M. Velický, K.Y. Tam, R.a.W. Dryfe, Hydrodynamic voltammetry at the liquid–liquid interface: application to the transfer of ionised drug molecules, *J. Electroanal. Chem.* 683 (2012) 94–102, <https://doi.org/10.1016/j.jelechem.2012.07.037>.
- [40] T. Cheng, Y. Zhao, X. Li, F. Lin, Y. Xu, X. Zhang, Y. Li, R. Wang, Computation of octanol - water partition coefficients by guiding an additive model with knowledge, *J. Chem. Inf. Model.* 47 (2007) 2140–2148, <https://doi.org/10.1021/ci700257y>.
- [41] T. Hinoue, E. Ikeda, S. Watariguchi, Y. Kibune, Thermal modulation voltammetry with laser heating at an aqueous|nitrobenzene solution microinterface: determination of the standard entropy changes of transfer for tetraalkylammonium ions, *Anal. Chem.* 79 (2007) 291–298, <https://doi.org/10.1021/ac061315l>.
- [42] D.W.M. Arrigan, Voltammetry of proteins at liquid–liquid interfaces, *Annu. Reports Sect. "C" (Physical Chem.* 109 (2013) 167, <https://doi.org/10.1039/c3pc90007j>.
- [43] E. Alvarez De Eulate, J. Strutwolf, Y. Liu, K. O'Donnell, D.W.M.M. Arrigan, An electrochemical sensing platform based on liquid–liquid microinterface arrays formed in laser-ablated glass membranes, *Anal. Chem.* 88 (2016) 2596–2604, <https://doi.org/10.1021/acs.analchem.5b03091>.
- [44] M. Nakamura, T. Osakai, Evaluation of the membrane permeability of drugs by ion-transfer voltammetry with the oil|water interface, *J. Electroanal. Chem.* 779 (2016) 55–60, <https://doi.org/10.1016/j.jelechem.2016.05.005>.
- [45] L.J. V Pidcock, Y.F. Jin, D.J. Griggs, *JAC Original articles Effect of hydrophobicity and molecular mass on the accumulation of fluoroquinolones by Staphylococcus aureus*, *J. Antimicrob. Chemother.* 47 (2001) 261–270.
- [46] K. Takacs-Novak, M. Józán, I. Hermecz, G. Szasz, Lipophilicity of antibacterial fluoroquinolones, *Int. J. Pharm.* 79 (1992) 89–96.
- [47] K. Bugyei, W.D. Black, S. McEwen, Pharmacokinetics of enrofloxacin given by the oral, intravenous and intramuscular routes in broiler chickens, *Can. J. Vet. Res.* 63 (1999) 193–200.
- [48] J. Biernacka, A.P. Mazurek, Experimental and theoretical studies on the molecular properties of ciprofloxacin, norfloxacin, pefloxacin, sparfloxacin, and gatifloxacin in determining bioavailability, *J. Biol. Phys.* 40 (2014) 335–345, <https://doi.org/10.1007/s10867-014-9354-z>.
- [49] D.L. Ross, S.K. Elkinton, C.M. Riley, *Physicochemical Properties of the Fluoroquinolone Antimicrobials. III. 1-Octanol-Water Partition Coefficients and Their Relationships to Structure*, vol. 88, 1992, pp. 379–389.
- [50] G.-M. Cardenas-Youngs, J.-L. Beltran, Dissociation constants and octanol – water partition equilibria for several fluoroquinolones, *J. Chem. Data.* 60 (2015) 3327–3332, <https://doi.org/10.1021/acs.jced.5b00556>.
- [51] T.L. Bidgood, M.G. Papich, Plasma and interstitial fluid pharmacokinetics of enrofloxacin, its metabolite ciprofloxacin, and marbofloxacin after oral administration and a constant rate intravenous infusion in dogs, *J. Vet. Pharmacol. Ther.* 28 (2005) 329–341.
- [52] M. Lizondo, M. Pons, M. Gallardo, J. Estelrich, Physicochemical properties of enrofloxacin, *J. Pharm. Biomed. Anal.* 15 (1997) 1845–1849, [https://doi.org/10.1016/S0731-7085\(96\)02033-X](https://doi.org/10.1016/S0731-7085(96)02033-X).
- [53] J.L. Davis, D. Little, A.T. Blikslager, M.G. Papich, Mucosal permeability of water-soluble drugs in the equine jejunum: a preliminary investigation, *J. Vet. Pharmacol. Ther.* 29 (2006) 379–385.
- [54] T. Grabowski, J.J. Jaroszewski, W. Piotrowski, Correlations between no observed effect level and selected parameters of the chemical structure for veterinary drugs, *Toxicol. In Vitro* 24 (2010) 953–959, <https://doi.org/10.1016/j.tiv.2010.01.003>.
- [55] Z. Liang, Z. Zhaob, T. Sun, W. Shi, F. Cui, Adsorption of quinolone antibiotics in spherical mesoporous silica: effects of the retained template and its alkyl chain length, *J. Hazard Mater.* 305 (2016) 8–14, <https://doi.org/10.1016/j.jhazmat.2015.11.033>.
- [56] VCCLAB, Virtual computational chemistry laboratory. <http://www.vcclab.org>, 2005.
- [57] A. Daina, O. Michielin, V. Zoete, SwissADME: a free web tool to evaluate pharmacokinetics, drug- likeness and medicinal chemistry friendliness of small molecules, *Sci. Rep.* 7 (2017) 1–13, <https://doi.org/10.1038/srep42717>.